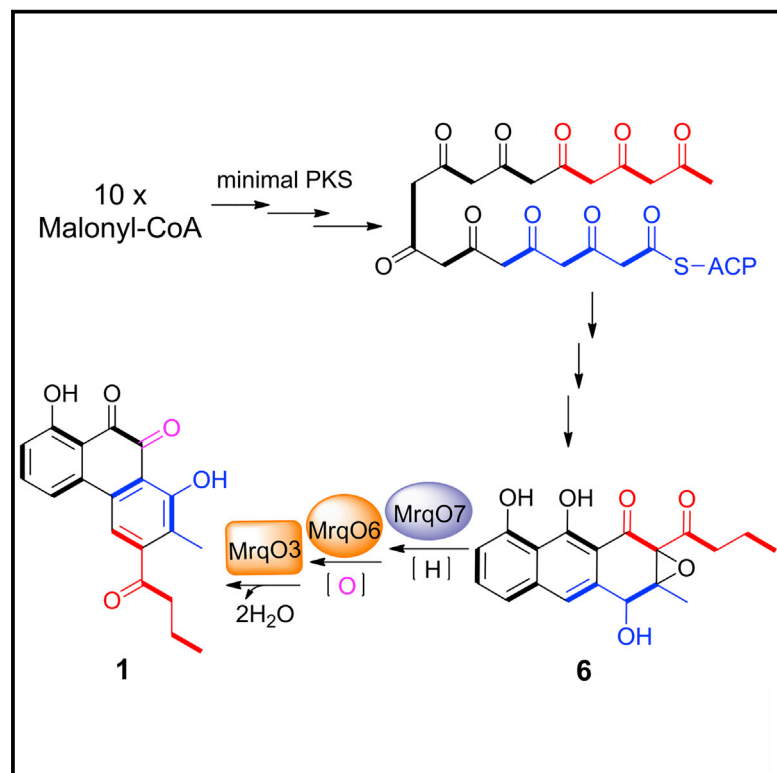


# Cell Chemical Biology

## Formation of an Angular Aromatic Polyketide from a Linear Anthrene Precursor via Oxidative Rearrangement

### Graphical Abstract



### Authors

Guixi Gao, Xiangyang Liu, Min Xu, ..., Ming Jiang, Shuangjun Lin, Meifeng Tao

### Correspondence

jiangming9722@sjtu.edu.cn (M.J.),  
linsj@sjtu.edu.cn (S.L.),  
tao\_meifeng@sjtu.edu.cn (M.T.)

### In Brief

Gao et al. discovered the formation of an angular 9,10-phenanthraquinone antibiotic from a linear tricyclic intermediate via oxidative rearrangement by three oxidoreductases, MrqO7, MrqO6, and MrqO3, proving a novel strategy for the biosynthesis of angular aromatic polyketides in nature.

### Highlights

- Identification of the entire murayaquinone biosynthetic gene cluster
- Anthrene-type model compounds were identified from biosynthetic mutants
- A linear 1(4*H*)-anthracenone epoxide is key intermediate for murayaquinone formation
- Three oxidoreductases catalyze skeleton rearrangement of the tricyclic intermediate

# Formation of an Angular Aromatic Polyketide from a Linear Anthrene Precursor via Oxidative Rearrangement

Guixi Gao,<sup>1</sup> Xiangyang Liu,<sup>1</sup> Min Xu,<sup>1</sup> Yemin Wang,<sup>1</sup> Fei Zhang,<sup>1</sup> Lijun Xu,<sup>1</sup> Jin Lv,<sup>1</sup> Qingshan Long,<sup>1</sup> Qianjin Kang,<sup>1</sup> Hong-Yu Ou,<sup>1</sup> Ying Wang,<sup>2</sup> Jürgen Rohr,<sup>3</sup> Zixin Deng,<sup>1</sup> Ming Jiang,<sup>1,\*</sup> Shuangjun Lin,<sup>1,\*</sup> and Meifeng Tao<sup>1,4,\*</sup>

<sup>1</sup>State Key Laboratory of Microbial Metabolism, Joint International Research Laboratory of Metabolic & Developmental Sciences, and School of Life Sciences and Biotechnology, Shanghai Jiao Tong University, Shanghai 200030, P. R. China

<sup>2</sup>Guangdong Province Key Laboratory of Pharmacodynamic Constituents of TCM and New Drugs Research, JNU-HKUST Joint Laboratory for Neuroscience and Innovative Drug Research, Jinan University, Guangzhou 510632, P. R. China

<sup>3</sup>Department of Pharmaceutical Sciences, College of Pharmacy, University of Kentucky, Lexington, KY 40536, USA

<sup>4</sup>Lead Contact

\*Correspondence: [jiangming9722@sjtu.edu.cn](mailto:jiangming9722@sjtu.edu.cn) (M.J.), [linsj@sjtu.edu.cn](mailto:linsj@sjtu.edu.cn) (S.L.), [tao\\_meifeng@sjtu.edu.cn](mailto:tao_meifeng@sjtu.edu.cn) (M.T.)

<http://dx.doi.org/10.1016/j.chembiol.2017.06.008>

## SUMMARY

Bacterial aromatic polyketides are a group of natural products synthesized by polyketide synthases (PKSs) that show diverse structures and biological activities. They are structurally subclassified into linear, angular, and discoid aromatic polyketides, the formation of which is commonly determined by the shaping and folding of the poly- $\beta$ -keto intermediates under the concerted actions of the minimal PKSs, cyclases and ketoreductases. Murayaquinone, found in several streptomycetes, possesses an unusual tricyclic angular aromatic polyketide core containing a 9,10-phenanthraquinone. In this study, genes essential for murayaquinone biosynthesis were identified, and a linear anthraoxirene intermediate was discovered. A unique biosynthetic model for the angular aromatic polyketide formation was discovered and confirmed through *in vivo* and *in vitro* studies. Three oxidoreductases, MrqO3, MrqO6, and MrqO7, were identified to catalyze the conversion of the linear aromatic polyketide intermediate into the final angularly arranged framework, which exemplifies a novel strategy for the biosynthesis of angular aromatic polyketides.

## INTRODUCTION

Polycyclic aromatic polyketides are a large group of natural products that show diverse chemical structures and a broad variety of biological activities such as anticancer, antibacterial, antifungal, and antiviral. Bacterial aromatic polyketides are generally synthesized by type II polyketide synthases (PKSs). A set of enzymes called minimal PKSs, consisting of the ketosynthase heterodimer ( $\beta$ -keto synthase, KS $_{\alpha}$ , and chain length factor, KS $_{\beta}$ ) and a free-standing acyl carrier protein (ACP), catalyze iterative Claisen condensations of ACP-tethered malonyl

units to generate a highly active poly- $\beta$ -ketoacyl thioester intermediate (McDaniel et al., 1994). Associated enzymes, including ketoreductases, cyclases, and aromatases, are required to direct the shaping and folding of the nascent poly- $\beta$ -ketoacyl thioester intermediate and convert it into a polyphenol intermediate with linear, angular, or discoid initial framework (Hertweck et al., 2007). The initial frameworks may undergo oxidative rearrangements, which are often catalyzed by Baeyer-Villiger oxygenases to afford modified skeletons, for example, the transformation of dehydrorabelomycin to the heterocyclic jadomycin and gilvocarcin skeletons (Rix et al., 2005; Tibrewal et al., 2012). In this way an initial linear framework might also be converted into an angular one, e.g., the proposed transformation of a linear anthracycline precursor to the dioxabenzo[a]pyrene ring system of the chartreusin aglycone (Xu et al., 2005). In addition, numerous tailoring enzymes catalyze diverse post-modification reactions, such as hydroxylations (Shen and Hutchinson, 1994; Koskiniemi et al., 2007), epoxidations (Maier et al., 2014), alkylations (Zhang et al., 2007), halogenations (Zhu et al., 2013), and glycosylations (Trefzer et al., 2000; Garrido et al., 2006), to eventually form more complex and biologically active natural products.

Murayaquinone is an angular aromatic polyketide antibiotic initially identified from *Streptomyces murayamaensis* in 1986 (Sato et al., 1986). It was subsequently isolated from several other unidentified *Streptomyces* species (Chu et al., 1996). Murayaquinone shares its 9,10-phenanthraquinone core with pilosquinone (Polonsky and Lederer, 1963) and haloquinone (Ewersmeyer-Wenk et al., 1981). Early feeding experiments using isotope-labeled precursors suggested a polyketide origin of murayaquinone, derived from ten acetate units via one-step decarboxylation. The unusual incorporation pattern of sodium [1,2-<sup>13</sup>C<sub>2</sub>]acetate and sodium [1-<sup>13</sup>C,<sup>18</sup>O<sub>2</sub>]acetate allowed to propose that murayaquinone was biosynthesized from a phenanthrene intermediate via oxidative rearrangement (Gould et al., 1997; Figure 1A).

In this work, we identified the murayaquinone biosynthetic gene cluster, and uncovered, through gene inactivation and enzyme studies, a novel biosynthetic route for the generation of angular aromatic polyketides (Figure 1B).

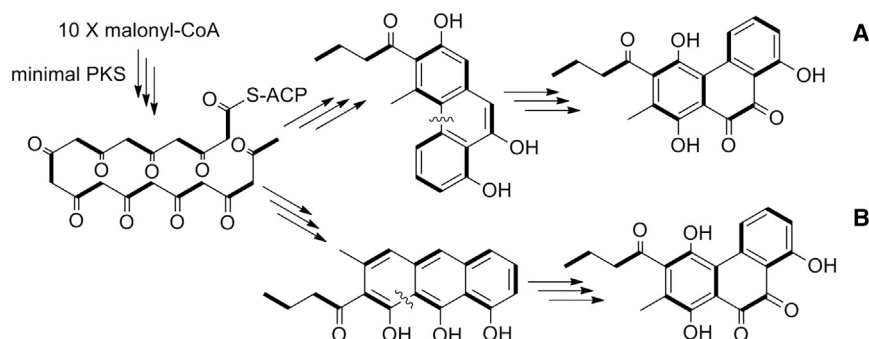


**Figure 1. Formation Model of Aromatic Polyketide Murayaquinone**

(A) Previously proposed formation of the angular murayaquinone.

(B) Confirmed formation of murayaquinone in this study.

## RESULTS

### Heterologous Production of Murayaquinone and Its Lactone Derivatives

*Streptomyces griseoruber* Sgr29 was isolated from soil in the Shennongjia forest in the Hubei province of China. Its fermentation broth showed no inhibition against bacterial indicator strains, such as *Staphylococcus aureus* or *Mycobacterium smegmatis*. However, *S. griseoruber* Sgr29 was subjected to our library expression and analysis (LEXAS) project for activation of silent biosynthetic gene clusters of antimicrobial metabolites in a surrogate host, *Streptomyces lividans* SBT5 (Xu et al., 2016), leading to the identification of three bacterial artificial chromosome (BAC) clones (3B4, 2E12, 6F3) that endowed the host with growth-inhibitory activity against *S. aureus* and *M. smegmatis*. All three exconjugants, SBT5/3B4, SBT5/2E12, and SBT5/6F3, produced the same distinguished peaks (**1**, **2**, and **3**) in high-performance liquid chromatography (HPLC) analyses (Figure 2A), suggesting that the three BAC clones shared the same biosynthetic gene cluster.

A 10-L fermentation of *S. lividans* SBT5/3B4, referred to as the wild-type (WT) strain in this study, allowed the purification and structural elucidation of the three compounds. Based on high-resolution mass spectrometry (HR-MS) data (Table S1) and  $^1\text{H}$  and  $^{13}\text{C}$  nuclear magnetic resonance (NMR) data (Table S2), **1** and **2** were determined to be murayaquinone and muraya-lactone, respectively, which were previously identified from *S. murayamaensis* (Sato et al., 1986; Melville and Gould, 1994). The HR-MS and NMR data suggested **3** to be an isomer of **2** (Figure 2B; Tables S1 and S2). Of critical importance were the assignments for C-8a and C-9a based on heteronuclear multiple bond correlation (HMBC). Correlations to C-8a (105.6 ppm) from H-5 (7.54 ppm) and H-7 (7.09 ppm) identified C-8a, which is linked to a carbonyl group. Correlation to C-9a (139.4 ppm) from H-4 (7.68 ppm) identified C-9a, which is attached to an oxygen atom (Table S2). The fact that compound **3** was found along with **1** and **2** indicated that it was biosynthesized in the same pathway. The structures of both **2** and **3** suggested these to be oxidative follow-up products of **1**.

### Identification of Essential Genes for the Biosynthesis of Murayaquinone

Sequencing of 3B4 yielded a circa 100-kb DNA region assumed to be responsible for the biosynthesis of murayaquinone, since it contained a minimal type II PKS gene set (*mrqA*, *mrqB*, and

reading frames (ORFs) related to secondary metabolism (Figure 3A).

To determine the essential genes for the biosynthesis of murayaquinone among these ORFs, we first determined the boundaries of *mrq* gene cluster by gene knockouts. Mutant  $\Delta\text{right}$  (removing circa 30 kb including  $\Delta\text{orf}25\text{--}28$ ) still produced **1–3** in amounts comparable with the WT strain (i.e., SBT5/3B4) (Figure 3B), while deletion of the adjacent gene *mrqL* resulted in a much higher production of **1** compared with the WT, and slightly lower production of **2** and **3** (Figure 4). Thus *mrqL* was determined as the right boundary of the gene cluster.

The determination of the left boundary of the *mrq* gene cluster was more complicated. Mutants  $\Delta\text{left}$  (removing 11.8 kb from *orf-3* to the insert-vector boundary),  $\Delta\text{orf-2}$ ,  $\Delta\text{orf-1}$ ,  $\Delta\text{orf}(1\text{--}2)$ ,  $\Delta\text{orf}23$ , and  $\Delta\text{orf}24$  still produced **1–3** in the same amounts as SBT5/3B4. However, mutant  $\Delta\text{RT}$  (removing 8 kb from *mrqT2-orf0*) abolished the production of **1–3**, which was unexpected (Figure 3B). Therefore this region, which contains two transporter genes (*mrqT1* and *mrqT2*) and two regulatory genes (*mrqR2* and *mrqR3*), was called the regulation region. Inactivation of *mrqO8* abolished the production of **1** and significantly reduced the production of **2** and **3** (Figure 4). Thus, the region between *mrqO8* and *mrqL* was named the biosynthesis region. Therefore, the *mrq* gene cluster includes two regions that are separated by an insertion of about 28-kb DNA, with a transposase-encoding gene *orf0* located at the left end of the insertion (Figure 3A).

In addition to the minimal PKS, the biosynthesis region encodes three ketoreductases (MrqF, MrqH, and MrqM), three cyclases (MrqD, MrqE, and MrqJ), eight oxidoreductases (MrqO1–O8), one regulator (MrqR1), and four hypothetical proteins (MrqG, MrqI, MrqK, and MrqL) (Table 1). To interrogate the genes necessary for the biosynthesis of **1–3**, single-gene deletion mutants were constructed, fermented, and analyzed by HPLC. The mutants were grouped roughly according to their abilities to produce **1–3** and to accumulate related compounds (Figures 4A–4D). Mutants  $\Delta\text{mrqE}$ ,  $\Delta\text{mrqF}$ ,  $\Delta\text{mrqG}$ ,  $\Delta\text{mrqM}$ , and  $\Delta\text{mrqO3}$  abolished the production of **1–3**, and did not accumulate any metabolites related to **1**, **2**, or **3** (Figure 4A). Mutants  $\Delta\text{mrqH}$ ,  $\Delta\text{mrqI}$ ,  $\Delta\text{mrqK}$ , and  $\Delta\text{mrqO2}$  still produced **2** and **3**, but also accumulated either one or two anthraquinone types of compounds, compounds **4** and **5**, respectively (Figure 4B).  $\Delta\text{mrqO4}$  and  $\Delta\text{mrqO5}$  also accumulated **4** and **5**, but abolished the production of **1–3**.  $\Delta\text{mrqO7}$  abolished the production of **1–3**, and accumulated another new metabolite, compound **6**, while  $\Delta\text{mrqO6}$  accumulated trace amounts of **5** and **6** (Figure 4C).

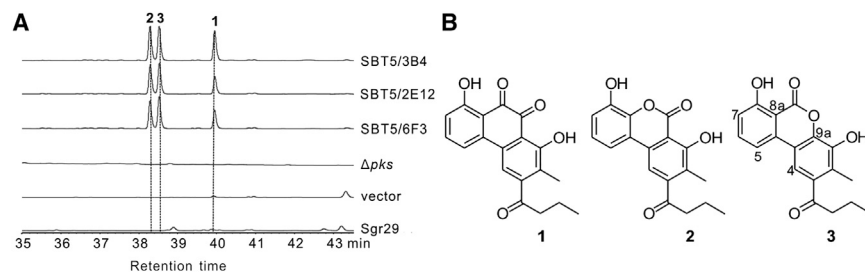


**Figure 2. Production of Murayaquinone and Its Derivatives by Heterologous Expression of Three BAC Clones Containing the *mrq* Gene Cluster**

(A) Heterologous production of murayaquinone **1** and murayalactones **2** and **3** in *S. lividans* SBT5 containing BAC clones. Note that there was no production of **1–3** in the native strain *S. griseoruber* Sgr29. The *pks* deletion mutant ( $\Delta pks$ ) and the vector control did not produce compounds **1–3**. HPLC traces were recorded at 280 nm.

(B) Chemical structures of murayaquinone **1** and murayalactones **2–3**.

$\Delta mrqD$  and  $\Delta mrqO8$  produced only trace amounts of **2** and **3**.  $\Delta mrqO1$  and  $\Delta mrqJ$  still produced **1–3** (Figure 4D). These findings confirmed all genes that partake in the production of **1–3** within the biosynthesis region, except for *mrqJ* and *mrqO1*.

### Structural Identification of the Metabolites Accumulated in the Mutants

The new peaks **4–6** were only accumulated by a few of the deletion mutants. The compounds were purified and their structures determined through MS and NMR spectroscopy. The structure of **4** was identified as mansoquinone by comparing the spectral data including HR-MS,  $^1\text{H}$ , and  $^{13}\text{C}$  NMR data with literature data (Figure 4E; Tables S1 and S3; Abdelfattah, 2009). The HR-MS of **5** suggested its molecular formula to be  $\text{C}_{19}\text{H}_{14}\text{O}_5$ , with a degree of unsaturation of 13, one more than that of **4**. This indicated **5** to contain either one more double bond or another ring. The  $^1\text{H}$  and  $^{13}\text{C}$  NMR data of **5** (Table S3) were almost identical to those of **4**. One obvious difference was that the methylene at C-13 position ( $\delta_{\text{H}} = 1.76$  and  $\delta_{\text{C}} = 17.1$ ) of **4** was changed to a methine in **5** ( $\delta_{\text{H}} = 4.78$  and  $\delta_{\text{C}} = 75.1$ ), which is linked to an oxygen atom, and that **5** contained only one phenolic hydroxyl proton forming an intramolecular hydrogen bond. Furthermore, the HMBC spectrum showed a correlation of this methine proton (H-13) to the aromatic carbon C-1 (Table S3). Thus, **5** was identified as a derivative of **4** with C-1 linking C-13 although an oxygen bridge, thereby forming an additional pyran ring (Figure 4E).

The molecular formula of **6** was determined as  $\text{C}_{19}\text{H}_{18}\text{O}_6$  by HR-MS, revealing that metabolite **6** contains one O atom more, but two H atoms less than **4** (Table S1). The  $^{13}\text{C}$ -NMR spectrum of **6** (Table S3) showed only ten aromatic carbons, two fewer than **4**, and only 2 carbonyl carbons, one fewer than **4**. There were three more carbons linked to oxygen, two of these are quaternary carbons ( $\delta_{\text{C}} = 66.5$  and  $68.7$ ) and one is a methine carbon ( $\delta_{\text{H}} = 4.98$  and  $\delta_{\text{C}} = 69.2$ ). The methyl group, which in **4** is attached to an aromatic ring ( $\delta_{\text{H}} = 2.37$  and  $\delta_{\text{C}} = 20.1$ ), is in **6** attached to a saturated carbon ( $\delta_{\text{H}} = 1.66$  and  $\delta_{\text{C}} = 16.4$ ). All these data combined led to structure **6**, which was further supported by 2D NMR spectra (Figure 4E; Table S3).

### Identification of Genes Responsible for the Formation of **1** from **6**

To check whether the compounds accumulated in the mutants are intermediates or shunt products in the murayaquinone biosynthetic pathway, we performed feeding experiments with compounds **4** and **6** to the  $\Delta pks$  mutant. We did not include

**5** in these studies, because of its much different structure, which likely rendered **5** as a shunt product. When compound **4** was fed, neither **1** nor **2** nor **3** were detected by HPLC analysis (Figure S1), while **1–3** were produced when **6** was fed to the same mutant (Figure 5A). These findings demonstrated that **4** is a shunt product, while **6** is an actual biosynthetic intermediate of murayaquinone.

The accumulation of **6** in  $\Delta mrqO7$  and  $\Delta mrqO6$  suggested that MrqO7 and MrqO6 played pivotal roles in the conversion of **6** into **1**. To further determine whether other genes encode additional enzymes involved in this conversion cascade, compound **6** was fed to seven single-gene deletion mutants that abolished the production of **1–3**. Compound **6** restored the production of **1–3** when fed to all of these mutants, for example the  $\Delta mrqG$  and  $\Delta mrqM$  mutants, except when fed to the  $\Delta mrqO3$  mutant (Figure 5A). This hinted that MrqO3 played a pivotal role in the conversion of **6** into **1**, along with MrqO6 and MrqO7. Sequence analysis suggested MrqO3 to be a putative cholesterol oxidase, MrqO6 to be a putative flavin adenine dinucleotide (FAD)-dependent monooxygenase homologous to BexE, and MrqO7 to be a putative NAD(P)-dependent oxidoreductase. Note that BexE was proposed to catalyze a Baeyer-Villiger reaction in the BE-7585A biosynthesis (Jackson et al., 2016).

### Biochemical Characterization of MrqO3, MrqO6, and MrqO7 Catalyzing Conversion of **6** to **1**

To uncover the mechanism of MrqO3, MrqO6, and MrqO7, which catalyze the conversion of **6** into **1**, these three oxidoreductases were expressed in *Escherichia coli* BL21(DE3). MrqO3 and MrqO6 were purified as bright yellow proteins, revealing the presence of a flavin prosthetic group, while MrqO7 was purified as a colorless protein. LC-MS analysis of the supernatant of denatured MrqO3 and MrqO6 proved the presence of FAD (Figure S2). Thereafter, we designed an *in vitro* assay system containing MrqO3, MrqO6, and MrqO7 in the presence of NADPH, NADH, and FAD, using **6** as a substrate. After the assay mixtures were incubated at  $30^\circ\text{C}$  for 60 min, **6** was completely converted to **1**, whereas the control reaction with boiled enzymes did not convert **6**. When any one of these three enzymes was removed from the assay, **1** was no longer detected, indicating that the cooperation of all three enzymes was essential for the conversion of **6** to **1**. The presence of either NADH or NADPH in the assay gave similar conversions of **6** to **1**, and **1** was not generated in absence of these co-factors, suggesting that the enzymes show no preference for NADH or

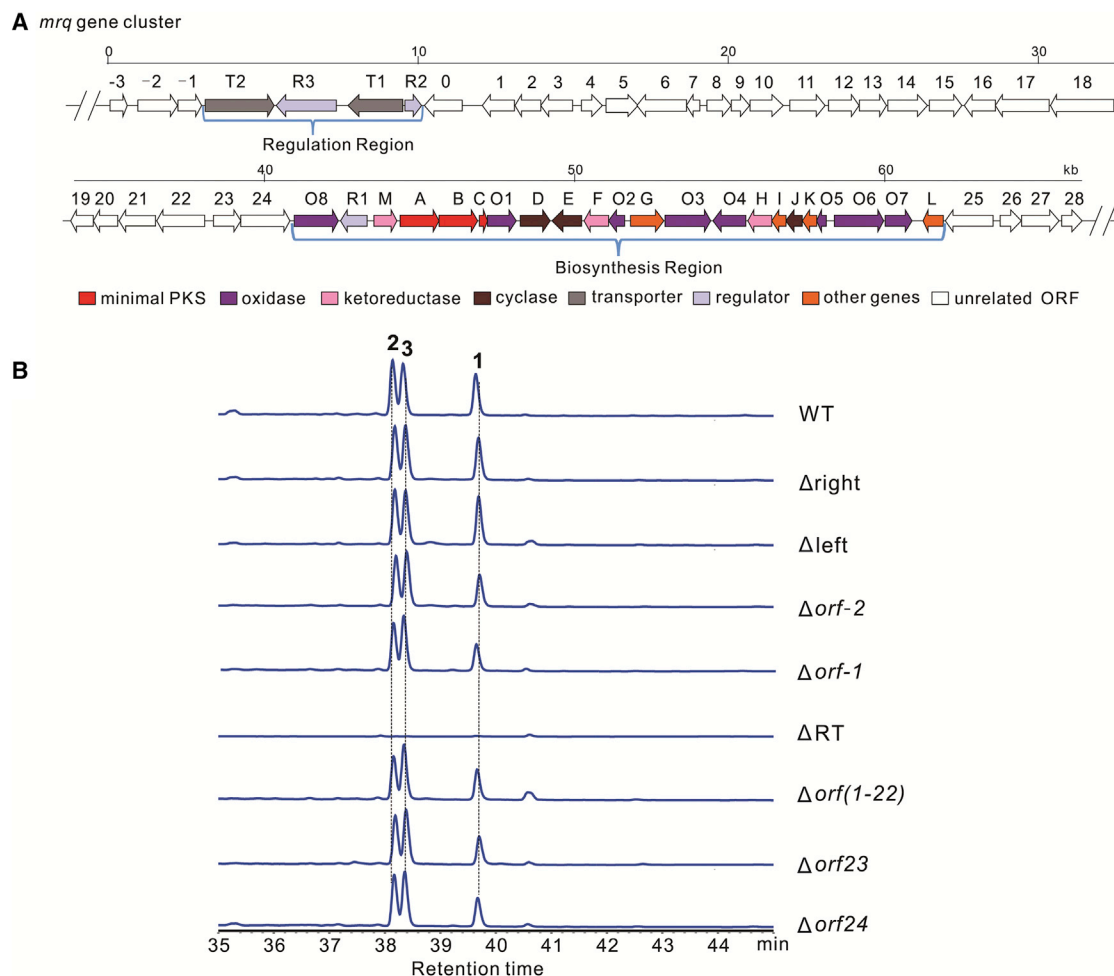


**Figure 3. Determination of the Boundaries of the *mrq* Gene Cluster by Deletions**

(A) Murayaquinone biosynthetic gene cluster in BAC 3B4.

(B) HPLC analysis of *S. lividans* SBT5/3B4 and its deletion mutants. Murayaquinone **1** and lactones **2** and **3** were produced by *S. lividans* SBT5/3B4 and all mutants except for  $\Delta$ RT. Note:  $\Delta$ RT was the mutant in which genes *mrqT2* to *orf0* were deleted.  $\Delta$ right, mutant in which a 30-kb fragment (including *orf25-orf28*) near the right boundary of the *mrq* gene cluster was deleted.  $\Delta$ left, mutant in which an 11.8-kb fragment (from *orf-3*) near the left boundary of the *mrq* gene cluster was deleted.

NADPH. However, the assay yielded similar conversions of **6** to **1** in the absence of exogenous FAD (Figure 5B), likely due to FAD bound to two of the proteins. Based on these findings, a time course study of the conversion of **6** to **1** catalyzed by the three enzymes was performed with 2  $\mu$ M of each enzyme, 1 mM of NADPH, and 360  $\mu$ M of **6**. Under these conditions **6** was completely converted to **1** within 30 min. In addition, since MrqO3 is a homolog of cholesterol oxidase, we also monitored H<sub>2</sub>O<sub>2</sub> production using the Fluorimetric Hydrogen Peroxide Assay Kit. No H<sub>2</sub>O<sub>2</sub> was detected in these reactions, indicating that H<sub>2</sub>O<sub>2</sub> was not formed.

Subsequently, the sequence of events involving each enzyme was investigated. For this, the *in vitro* assay was changed, now using each enzyme individually in the presence of NADPH and **6**. The reactions were carried out by incubation at 30°C for 30 min, and LC-MS was used to monitor the formation of possible products (Figure 5C). The reaction with MrqO3 did not show any conversion of substrate **6**. The reaction with MrqO6

generated an obvious new ion peak at  $m/z$  381.3 ([M + Na]<sup>+</sup>, 16 Da more than that of **6** (365.3, [M + Na]<sup>+</sup>), indicating one oxygen atom to be inserted into **6**, resulting in structures **7** or **7'** in Figure 6. When MrqO7 was used in the assay, the LC-MS analysis revealed a new ion peak at  $m/z$  367.3 ([M + Na]<sup>+</sup>, 2 Da more than that of **6**, indicating an addition of two hydrogen atoms, consistent with a reduced product, e.g., intermediate **8**. These results indicated that both MrqO6 and MrqO7 could recognize **6** as substrate, while MrqO3 catalyzed the following last step of the conversion of **6** to **1**.

To further clarify the catalytic order involving MrqO7 and MrqO6 during the conversion of **6** to **1**, we carried out three parallel sequential reactions SR-I, SR-II, and SR-III. The sequential reactions were all run in a two-step manner with the MrqO7-catalyzed reduction or the MrqO6-catalyzed Baeyer-Villiger reaction separately set as alternative first steps, while MrqO3 was always involved in the following second step. After the first-step reaction, the enzyme was removed by

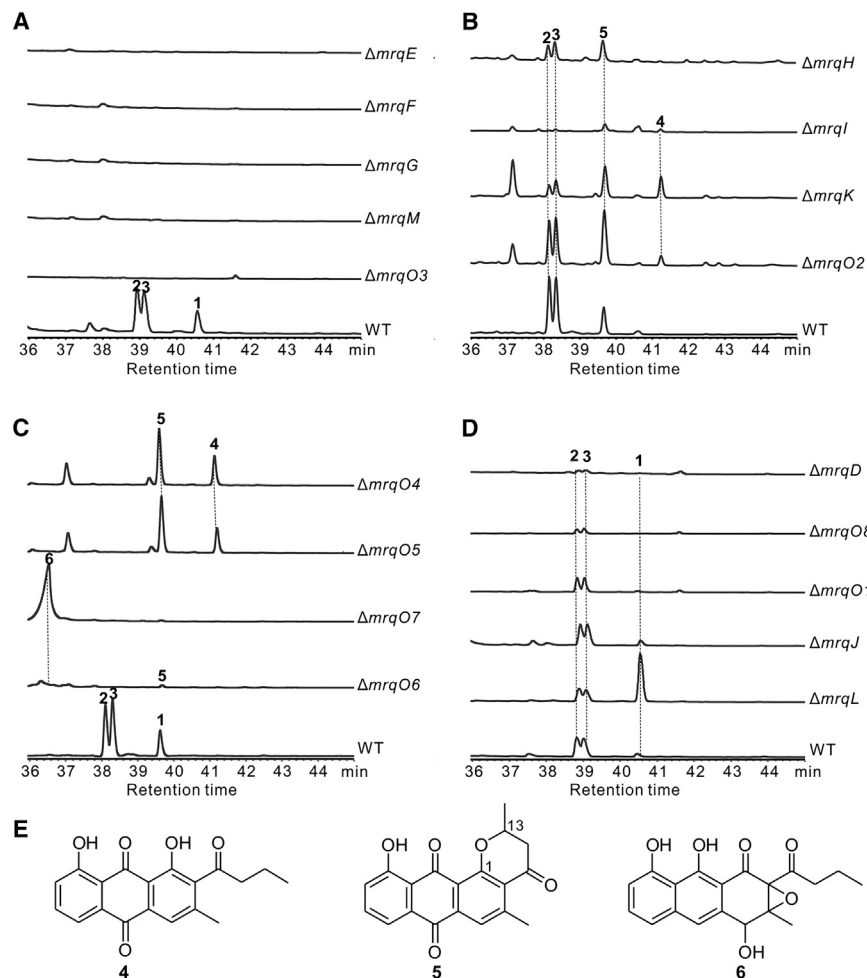


**Figure 4. Metabolite Profiles of the Single-Gene Deletion Mutants of the *mrq* Gene Cluster**

(A) No metabolite was detected in mutants  $\Delta mrqE$ ,  $\Delta mrqF$ ,  $\Delta mrqG$ ,  $\Delta mrqM$ , and  $\Delta mrqO3$ . (B) Accumulation of both angular compounds 1–3, and the anthraquinone-type compounds 4 and 5, in  $\Delta mrqH$ ,  $\Delta mrqI$ ,  $\Delta mrqK$ , and  $\Delta mrqO2$ . (C) Accumulation of anthraquinones 4 or 5, or anthrone 6, in  $\Delta mrqO4$ ,  $\Delta mrqO5$ ,  $\Delta mrqO6$ , and  $\Delta mrqO7$ . (D) Production of 1–3 in  $\Delta mrqD$ ,  $\Delta mrqO8$ ,  $\Delta mrqO1$ ,  $\Delta mrqJ$ , and  $\Delta mrqL$ . (E) Chemical structures of 4–6.

eton (Brockmann and Reschke, 1968; Brockmann et al., 1969; Ishida et al., 2006; Fritzsche et al., 2008). The formation of the linear or angular architecture of bacterial aromatic polyketides from poly- $\beta$ -keto intermediates is proposed to result from the concerted actions of minimal PKSs and associated ketoreductases, cyclases, and aromatases (Hertweck et al., 2007). Surprisingly, several angular aromatic polyketides, such as the anticancer agent BE-7585A, the antibiotic murayaquinone, and chartreusin, displayed unexpected, atypical polyketide labeling patterns from  $^{13}\text{C}$ -acetate feeding experiments (Sasaki et al., 2010; Gould et al., 1997; Canham and Vining, 1976; Canham et al., 1977). Therefore, these angular aromatic polyketides were proposed to

filtering, which was confirmed using the Bradford Protein Assay Kit. Subsequently, the second step was initiated through addition of the other two enzymes. In SR-I, the MrqO7-catalyzed hydrogenation was set as the first-step reaction, while the MrqO6-catalyzed Baeyer-Villiger reaction was set as the first-step reaction in SR-II. The complete conversion of **6** to **1** catalyzed by all three enzymes was used as the positive control in SR-III. HPLC analysis showed that the production of **1** in SR-I was similar to that observed in the positive control, much higher than that in SR-II (Figure S3). These observations unambiguously verified that the reductive epoxide opening of **6** catalyzed by MrqO7 occurs prior to the MrqO6-catalyzed Baeyer-Villiger reaction.

## DISCUSSION

Bacterial aromatic polyketides are an important class of natural products because of their diverse chemical structures and bioactive properties. On the basis of the polyphenolic ring system, aromatic polyketides were classified into several different subclasses such as anthracyclines, angucyclines, and tetracyclines (Zhan, 2009). These natural products possess either a linear- or an angular-shaped core structure, with the exception of resistomycin and resistoflavin, which have a discoid skel-

arise from oxidative rearrangements of linear polyphenolic intermediates, involving C-C bond cleavage and new C-C bond formation. Indeed, a linear anthracyclic metabolite, resomycin C, was accumulated upon inactivation of ChaZ, a Baeyer-Villigerase-like FAD-dependent oxygenase of the chartreusin biosynthesis. However, ChaZ was found unable to convert resomycin C (Xu et al., 2005). In the BE-7585A biosynthetic pathway, three oxygenases (BexE, BexI, and BexM) had been proposed to catalyze the oxidative rearrangement of an unidentified linear anthracyclinone intermediate to generate an angular angucyclinone intermediate in the biosynthesis of anticancer agent BE-7585A (Sasaki et al., 2010). Most recently, the crystal structure of BexE was resolved to 2.65 Å and used to perform docking simulations to determine the key linear intermediate. However, unfortunately, the identification of BexE's true substrate remains challenging (Jackson et al., 2016). In contrast, in this work on murayaquinone biosynthesis, we proved and confirmed the conversion of a linear polyphenolic intermediate to an angular aromatic polyketide.

## Characterization of the *mrq* Gene Cluster and the Murayaquinone Biosynthetic Pathway

The entire biosynthetic gene cluster was cloned and expressed in the heterologous host *S. lividans* SBT5 utilizing the previously

**Table 1. Deduced Function of the Gene Products of the *mrq* Gene Cluster**

Proteins (aa)	Proposed Function	Homologs (Sequence ID in NCBI, Origin)	Identity/Similarity (%)
<b>Regulation Region</b>			
MrqT2 (725)	Transporter	WP_023423080.1, <i>S. sp.</i> GBA 94-10	57/69
MrqR3 (644)	Regulator	WP_051823225.1, <i>S. sp.</i> NRRL S-1448	42/56
MrqT1 (574)	transporter	WP_063760793.1, <i>S. aureocirculatus</i>	78/86
MrqR2 (177)	regulator	WP_051852929.1, <i>S. aureocirculatus</i>	73/86
<b>Biosynthesis Region</b>			
MrqO8 (471)	oxygenase/dehydratase	JadH, <i>S. venezuelae</i>	38/48
MrqR1 (266)	regulator	WP_020939953.1, <i>S. collinus</i>	52/68
MrqM (245)	3-oxoacyl-ACP reductase	SsfK, <i>S. sp.</i> SF2575	51/67
MrqA (417)	KS <sub>α</sub>	PgaA, <i>S. sp.</i> PGA64	80/86
MrqB (414)	KS <sub>β</sub>	ChaB, <i>S. chartreusis</i>	70/80
MrqC (87)	ACP	AGO50612.1, <i>S. lusitanus</i>	51/67
MrqO1 (308)	oxidoreductase	AHL46730.1, <i>S. bottropensis</i>	56/66
MrqD (319)	second ring cyclase	AlnR, <i>S. sp.</i> CM020	58/69
MrqE (317)	cyclase	PgaL, <i>S. sp.</i> PGA64	57/69
MrqF (262)	polyketide C-9 ketoreductase	PgaD, <i>S. sp.</i> PGA64	71/80
MrqO2 (172)	flavin reductase	AHL46683.1, <i>S. bottropensis</i>	32/51
MrqG (356)	unknown	WP_067167737.1, <i>S. sp.</i> ERV7	78/82
MrqO3 (489)	FAD-binding oxidoreductase	WP_030637315.1, <i>S. flavovirens</i>	49/64
MrqO4 (351)	oxidase	AHL46682.1, <i>S. bottropensis</i>	61/76
MrqH (256)	ketoreductase	MtmTIII, <i>S. argillaceus</i>	58/66
MrqI (153)	unknown	WP_049531873.1, <i>Streptococcus pseudopneumoniae</i>	31/44
MrqJ (177)	cyclase	AknE1, <i>S. galilaeus</i>	46/60
MrqK (154)	unknown	WP_067167164.1, <i>S. sp.</i> ERV7	75/84
MrqO5 (103)	oxygenase	ChaH, <i>S. chartreusis</i>	43/58
MrqO6 (532)	FAD-binding monooxygenase	BexE, <i>Amycolatopsis orientalis</i> ssp. <i>vinearia</i>	29/38
MrqO7 (287)	NAD(P)-dependent oxidoreductase	WP_040811703.1, <i>Nocardia concava</i>	53/63
MrqL (216)	unknown	WP_004941039.1, <i>S. mobaraensis</i>	46/61

described LEXAS technology (Xu et al., 2016), because the natural strain *S. griseoruber* Sgr29 did not produce murayaquinone. The 28-kb *mrq* gene cluster consists of two parts, a regulation/efflux region and a biosynthesis region, separated by an insertion of a 28-kb unrelated fragment implied to have originated horizontally (evident from the presence of a transposase gene *orf0*; Figure 3A).

The murayaquinone biosynthesis pathway was updated after a bioinformatics analysis, genetic studies, and compound production from gene deletion mutants (Figure 6A). The generation of the first tricyclic aromatic intermediate (**10**) was proposed based on the typical biosynthetic logic of PKS II for the synthesis of some decaketides via C-9 ketoreduction and C-7-C-12 first ring cyclization, such as nogalonic acid (Kantola et al., 2000; Hautala et al., 2003), tetracycline SF2575 (Pickens et al., 2009), and mensacarcin (Maier et al., 2015). Besides the minimal PKS, the sequences of ketoreductase MrqF, and of the two cyclases MrqE and MrqD, were highly similar to SnoaD/SsfU/MsnO11, SnoaE/SsfY1/MsnC3, and SsfY2/MsnC2, respectively, which were responsible for the C-9 ketoreduction, C-7 to C-12 first ring cyclization, and second/third ring cyclization, respectively.

Subsequent modifications of **10**, by MrqH, MrqO8, MrqI, MrqK, MrqO5, MrqO1, and MrqO4, led to the production of key intermediate **6** (Figure 6A). MrqH, a ketoreductase homolog, was proposed to catalyze the reduction of the keto group for the butyryl side chain formation of **11**. Since the distant keto group of **10** can possibly be reduced, less effectively, by ketoreductases from the host, traces of murayaquinone and the murayalactones can be detected as products of the  $\Delta mrqH$  mutant. However, in the absence of MrqH, **10** reacts predominantly spontaneously, initially to form a pyrone ring by cyclization and dehydration, followed by other spontaneous reactions, an oxidation to form the anthraquinone, reduction of the pyrone lactone to a hemiacetal likely through a hydrogenase from the host (McDaniel et al., 1994; Fu et al., 1994), to eventually produce **5** (Figure 4B).

MrqO8 is an FAD-binding motif-containing protein showing homology to JadH that catalyzes dehydration and oxidation in the jadomycin biosynthetic pathway (Chen et al., 2005, 2010), so it was speculated to participate in the formation of the first aromatic ring or the conversion of **11** to **12** by dehydration (Figure 6A). Its inactivation mutant still produced murayaquinone and murayalactones, but with drastically decreased production

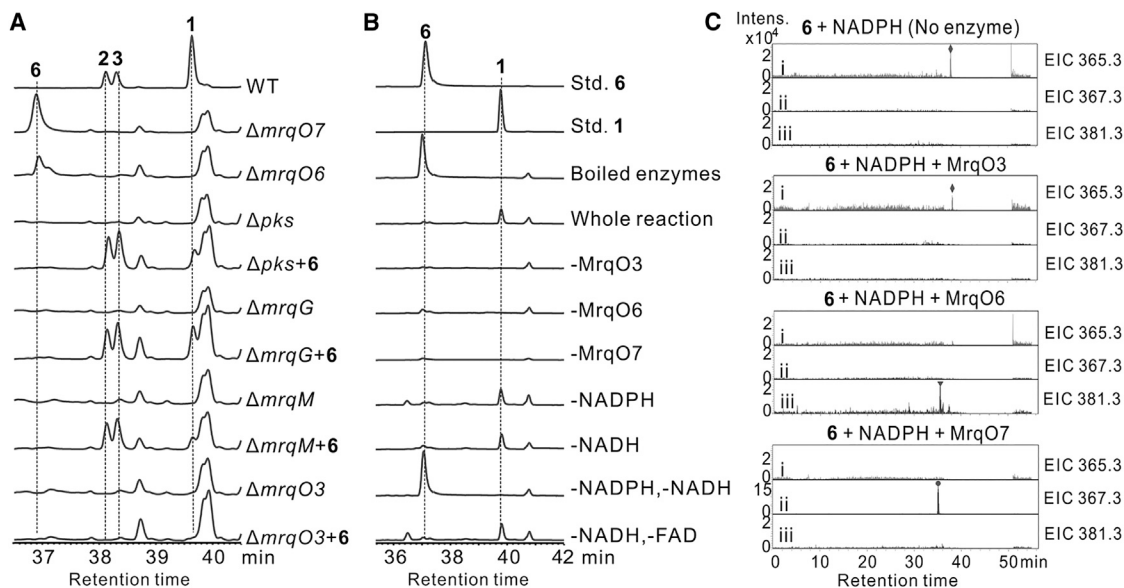


**Figure 5. In Vivo and In Vitro Characterization of the Conversion of 6 to 1**

(A) Detection of *in vivo* conversions in four mutants. Compound **6** was converted to **1–3** in  $\Delta pks$ ,  $\Delta mrqG$ , and  $\Delta mrqM$ , but not in  $\Delta mrqO3$ . The WT strain (SBT5/3B4) producing **1–3** and two mutants producing **6** ( $\Delta mrqO7$  and  $\Delta mrqO6$ ) were used as controls to indicate the peaks.

(B) Biochemical conversion of **6** to **1** with different combinations of enzymes and co-factors. All reactions were conducted at 30°C for 60 min. The complete reaction sequence was achieved by a mixture of three enzymes (MrqO3, MrqO6, and MrqO7), three co-factors (NADPH, NADH, and FAD), and the substrate **6**. Other reactions were the same mixtures as for the complete reaction sequence except for the indicated omission, for example, –MrqO3 means minus MrqO3 from the complete reaction mixture. HPLC traces were recorded at 280 nm.

(C) LC-MS analysis of the enzymatic conversion of **6** by single proteins. Compound **6** (246  $\mu$ M) was incubated with no enzyme, MrqO3 (2  $\mu$ M), MrqO6 (2  $\mu$ M), or MrqO7 (2  $\mu$ M), in the presence of NADPH at 30°C for 30 min, and the samples were detected immediately. (i)–(iii) Show the extracted ion chromatogram (EIC) of 365.3, 367.3, and 381.3, which are the *m/z* ( $[M + Na]^+$ ) values of the substrate (compound **6**), the +2 Da intermediate, and the +16 Da intermediate, respectively.

levels compared with the WT strain, probably due to spontaneous dehydration (Figure 4D).

MrqI and MrqK are NTF2-like superfamily small proteins with a SnoaL\_2 and SnoaL\_4 domain, respectively (Marchler-Bauer et al., 2016). The metabolic profiles of MrqI- and MrqK-inactivation mutants were very similar, except that the compound production in  $\Delta mrqI$  was much lower. Both  $\Delta mrqI$  and  $\Delta mrqK$  mutants accumulated **4** and **5** while decreasing production of **2** and **3** (Figure 4B). Taken together, MrqI and MrqK may take part in the reduction of **12** to **13**, or reduce the keto group of **15** to form the hydroxyl of **6** (Figure 6A).

The formation of **6** from **13** also involves three oxidation steps catalyzed by MrqO5, MrqO1, and MrqO4 (Figure 6A). This was proposed based on bioinformatics analysis (Table 1) and metabolic profiling of their inactivation mutants (Figures 4C and 4D).

### Biochemical Characterization of the Conversion of the Linear Intermediate **6** to the Angular Product Murayaquinone

The accumulation of anthrene-type compounds (**4**, **5**, and **6**) in several mutants indicates that a linear anthrene-type compound, not the previously proposed angular phenanthrene, may be the true substrate of the oxidative rearrangement to form the angular murayaquinone. Biotransformation of **6** to **1** in the PKS-inactivation mutant suggested **6** to be an actual intermediate of the biosynthetic pathway of **1**. Accumulation of **6** in the  $mrqO6$  and  $mrqO7$  deletion mutants suggested that these two genes encoded enzymes for the **6** to **1** conversion.

The enzymatic conversion of **6** to **1** was then investigated. Since both the MrqO6- and MrqO7-inactivation mutants accumulated compound **6**, this compound should generally be the substrate of either MrqO6 or MrqO7. MrqO6 is an FAD-dependent monooxygenase, with 29% identity and 38% similarity to BexE, which has been proposed to catalyze a Baeyer-Villiger reaction in BE-7585A biosynthesis, and MrqO7 is an NAD(P)-dependent oxidoreductase. Unfortunately, when **6** was incubated with MrqO6 or MrqO7, or both MrqO6 and MrqO7, **6** was consumed and many tiny peaks were detected by HPLC (Figure S4), indicating unstable products, consistent with the findings for BexE and BexF (Jackson et al., 2016), although MrqO7 shows no homology to BexF. Thus, as proposed for BexE and BexF, **6** might be converted to a very unstable compound through MrqO6 and/or MrqO7, and is readily degraded or oxidized to generate several other compounds. Therefore, we assumed that an/other enzyme/s may cooperate closely with MrqO6 and MrqO7 to convert the unstable product of MrqO6 and MrqO7 into a stable compound. But this/these enzyme/s may not accept **6** as the substrate. On the basis of this assumption, **6** was fed to the deletion mutants that did not produce **1–3**, with the PKS-inactivation mutant as a positive control. This way, MrqO3, a predicted cholesterol oxidase homolog, was identified as a candidate cooperating with MrqO6 and MrqO7. Indeed, when MrqO3, MrqO6, and MrqO7 were incubated with **6** in the presence of FAD and NADPH, **6** was successfully converted to **1** within 30 min.

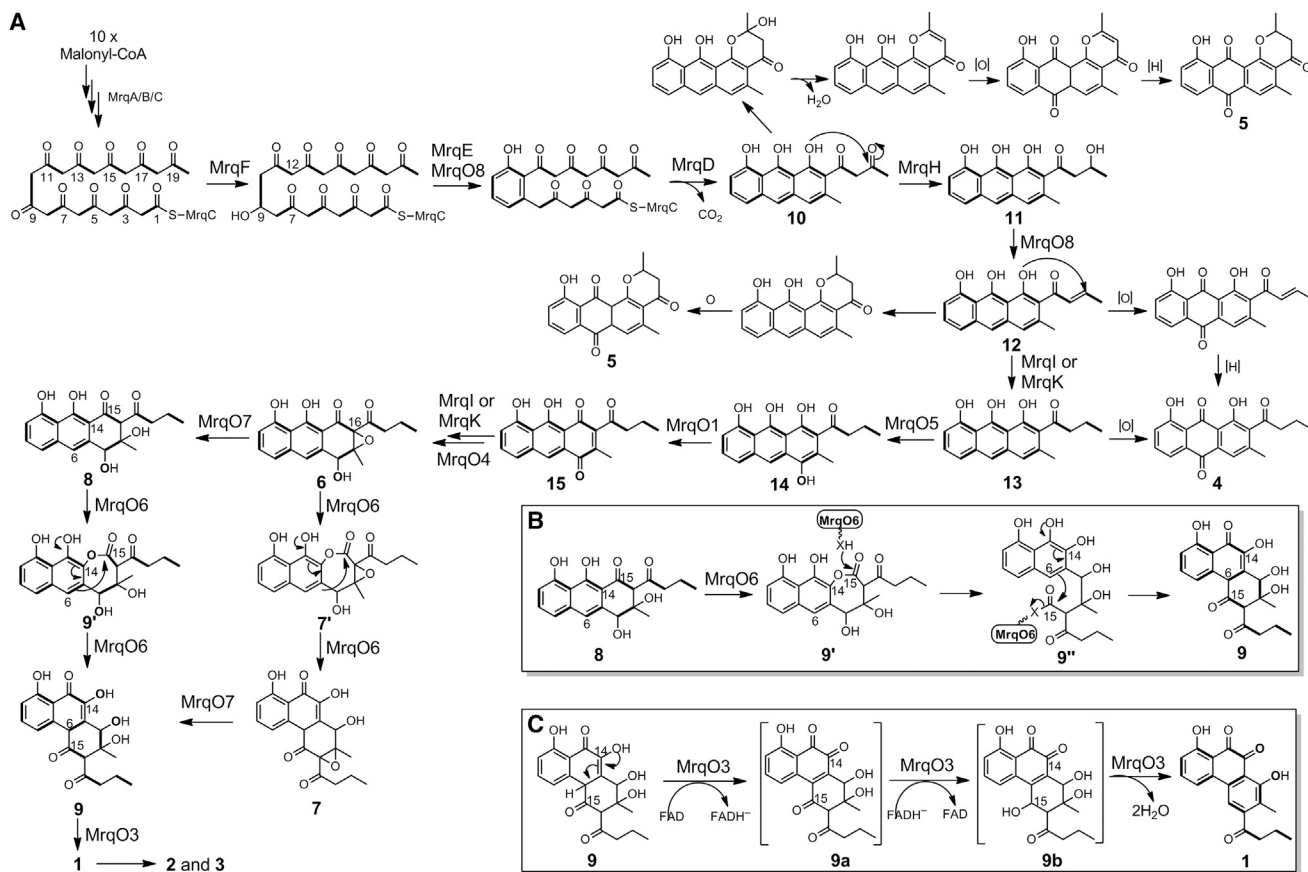


**Figure 6. Proposed Biosynthesis of 1–3**

(A) Proposed biosynthetic pathway of murayaquinone **1** and its lactone derivatives **2** and **3**.

(B) Proposed enzymatic mechanism of the oxidative rearrangement catalyzed by MrqO6.

(C) Proposed enzymatic mechanism of the conversion of **9** to **1** catalyzed by MrqO3.

The order in which MrqO6 and MrqO7 act during the **6** to **1** conversion was determined by sequential enzymatic reactions. It was clearly demonstrated that the MrqO7-catalyzed hydrogenation on **6** is the first step, followed by the reactions of MrqO6 and MrqO3 to afford the final product **1**. Some remaining questions were also addressed by these experiments: (1) MrqO6 may not interact with MrqO7 and no complex should be formed, which is different from the previous speculation (Jackson et al., 2016); (2) the products of MrqO7 and MrqO6 seem to be stable enough in the reaction mixture to allow the follow-up conversion steps to **1**, but they readily decompose during the work-up process.

When LC-MS was used to follow the reactions catalyzed by MrqO6 and MrqO7, respectively, possible products can be detected and the type of the reactions can also be deduced from mass spectral analysis. The mass of the product **7/7'** from MrqO6 is 16 Da greater than **6**, indicating a single oxygen atom to be inserted into **6**, consistent with a Baeyer-Villiger reaction, such as those proposed for ChaZ (Xu et al., 2005) or BexE (Jackson et al., 2016). The mass of product **8** from MrqO7 is 2 Da greater than **6**, and NAD(P)H is necessary for its formation, indicating that two protons were added to **6**, and that the reaction catalyzed by MrqO7 is a reduction. On the basis of the nature

of reductive reactions and the structure of the final product **1**, we proposed that the hydride from NAD(P)H attacks C-16 to form a vicinal diol **8**. The formation of **6** and **8** is probably intended to disrupt the aromatic ring and enable the Baeyer-Villiger reaction. To some extent, this may explain why the aromatic resomycin C is not a substrate of ChaZ (Xu et al., 2005). As proposed above, the MrqO6-catalyzed Baeyer-Villiger reaction disrupts the C-C bond between C-14 and C-15 by insertion of an oxygen atom. Since C-6 cannot directly attack the carbonyl C-15 due to the spatial tension and hindrance, a thiol of a cysteine residue or a carboxyl group of MrqO6 may function as a nucleophile to attack C-15, generating an enzyme bound thioester or anhydride intermediate, as shown in Figure 6B. Thioesters are commonly used for an activation of a carboxyl carbon in PKs and non-ribosomal peptide synthetases, the most similar example being KSs that use cysteine to load and activate the carboxyl carbons (Bisang et al., 1999; Robbins et al., 2016; Walsh, 2016). Anhydrides are also very commonly used for carboxyl carbon activation, both chemically and enzymatically. For example, adenylation enzymes use acyl adenylation, and some amidases use acyl adenylation or phosphorylation, to activate carboxyl carbons (Begley et al., 2001; Gulick, 2009). It is very possible that a nucleophilic residue attacks C-15 to form

a linear anhydride such as **9'**, and the electron-rich C-6 subsequently attacks the C-15 of **9'** to form the new C-C bond of **9**.

MrqO3 is a homolog of cholesterol oxidase. Cholesterol oxidases are a type of flavoenzymes that catalyze oxidation and isomerization of cholesterol in the first step of a metabolic pathway for utilizing cholesterol as a carbon and energy source (Murooka and Yamashita, 2001). Cholesterol oxidases catalyze the oxidation of cholesterol. During this reaction, the co-factor FAD is converted to FADH<sub>2</sub>, which, in turn is spontaneously oxidized by aerial oxygen to generate H<sub>2</sub>O<sub>2</sub> and to recycle FAD (Yue et al., 1999; Lario et al., 2003). In the assays catalyzed by the mentioned three enzymes, no H<sub>2</sub>O<sub>2</sub> was detected using the Fluorimetric Hydrogen Peroxide Assay Kit, suggesting that MrqO3 may catalyze oxidative and reductive reactions, accompanying the loss of two molecules of water, to eventually form the final product **1** (Figure 6C). First, FAD subtracts the hydride from **9** to generate FADH<sup>-</sup> and **9a**. FADH<sup>-</sup> subsequently transfers the hydride to the carbonyl carbon C-15 to perform the reductive reaction to form **9b**, thereby recycling FAD, distinct from the typical reactions catalyzed by cholesterol oxidases mentioned above. The loss of water of **9b** is very likely catalyzed by MrqO3, but a spontaneous dehydration cannot be ruled out.

## SIGNIFICANCE

**Angular aromatic polyketides are a subtype of aromatic bacterial polyketide natural products. Some of these are oxidatively rearranged from initially formed linear intermediates through an FAD-dependent Baeyer-Villiger oxygenase. However, only little biochemical evidence has been obtained to support this. In this study we demonstrated, *in vivo* and *in vitro*, that three oxidoreductases cooperate to catalyze the conversion of a linear tricyclic intermediate to the angular 9,10-phenanthraquinone. In the *in vitro* studies, the cholesterol oxidase homolog MrqO3 played an important role to convert an unstable intermediate to a chemically stable final product. Based on the sequence alignment of the three oxidoreductases, hypotheses for an oxidative rearrangement involving a Baeyer-Villiger reaction were proposed and interrogated. Overall, the studies revealed a novel strategy for the biosynthesis of angular aromatic polyketides.**

## STAR★METHODS

Detailed methods are provided in the online version of this paper and include the following:

- KEY RESOURCES TABLE
- CONTACT FOR REAGENT AND RESOURCE SHARING
- EXPERIMENTAL MODEL AND SUBJECT DETAILS
  - Bacterial Strains
  - Plasmids
  - Culture Conditions
- METHODS DETAILS
  - Construction and Screen of the Genomic BAC Library of *S. griseoruber* Sgr29
  - Construction of Large Deletion Mutants and Single Gene Deletion Mutants

- Purification of Compounds 1-3 from *S. lividans* SBT5/3B4
- Purification of Compounds 4 and 5 from *S. lividans* SBT5/3B4ΔmrqO4
- Purification of Compound 6 from *S. lividans* SBT5/3B4ΔmrqO7
- In Vivo Conversion of 6 to 1 by Feeding 6 to Mutants during Fermentation
- Feeding 4 to the Δpks Mutant during Fermentation
- Expression, Purification and Analysis of MrqO3, MrqO6 and MrqO7
- Determination of the Catalytic Order of MrqO6 and MrqO7
- Detection of H<sub>2</sub>O<sub>2</sub> in the In Vitro Conversion of 6 to 1 Catalyzed by MrqO7, MrqO6 and MrqO3
- QUANTIFICATION AND STATISTICAL ANALYSIS
- DATA AND SOFTWARE AVAILABILITY
  - Data Resources

## SUPPLEMENTAL INFORMATION

Supplemental Information includes four figures, three tables, and NMR spectra and can be found with this article online at <http://dx.doi.org/10.1016/j.chembiol.2017.06.008>.

## AUTHOR CONTRIBUTIONS

M.T., S.L., M.J., and Z.D. designed the research; G.G., X.L., M.X., Y.W., F.Z., L.X., J.L., and Q.L. performed the research; M.T., S.L., M.J., J.R., Q.K., H.-Y.O., G.G., and Y.W. analyzed the data; M.T., S.L., M.J., G.G., and J.R. wrote the paper.

## ACKNOWLEDGMENTS

We thank Songwang Hou, Tianshen Tao, and Colin P. Smith for gifts of bacterial strains. This work was supported by NSF (31370134, 31425001, 31300033, and 21661140002) of China, and the MOST (2012CB721000; 2010AA10A201; Chinese-Australia Joint Grant: 2016YFE0101000), the US NIH (grant R01 GM 105977), and the Science and Technology Commission of Shanghai Municipality (15JC1400401).

Received: February 16, 2017

Revised: April 28, 2017

Accepted: June 16, 2017

Published: July 13, 2017

## REFERENCES

- Abdelfattah, M.S. (2009). Mansoquinone: isolation and structure elucidation of new antibacterial aromatic polyketides from terrestrial *Streptomyces* sp. Eg5. *Nat. Prod. Res.* 23, 212–218.
- Bai, T., Yu, Y., Xu, Z., and Tao, M. (2014). Construction of *Streptomyces lividans* SBT5 as an efficient heterologous expression host. *J. Huazhong Agric. Univ.* 33, 1–6.
- Begley, T.P., Kinsland, C., and Strauss, E. (2001). The biosynthesis of coenzyme A in bacteria. *Vitam. Horm.* 61, 157–171.
- Bisang, C., Long, P.F., Corte, J., Westcott, J., Crosby, J., Matharu, A.-L., Cox, R.J., Simpson, T.J., Staunton, J., and Leadlay, P.F. (1999). A chain initiation factor common to both modular and aromatic polyketide synthases. *Nature* 401, 502–505.
- Brockmann, H., and Reschke, T. (1968). The composition of resistomycin. *Tetrahedron Lett.* 3167–3170.

- Brockmann, H., Meyer, E., Schrempf, K., Einers, F., and Reschke, T. (1969). Resistomycin. IV. The constitution of resistomycins. *Chem. Ber.* **102**, 1224–1246.
- Canham, P., and Vining, L.C. (1976). Pattern of acetate incorporation into the aglycone of chartreusin. Evidence from  $^{13}\text{C}$  nuclear magnetic resonance studies for a single-chain polyketide intermediate. *J. Chem. Soc. Chem. Commun.* **169**, 319–320.
- Canham, P.L., Vining, L.C., McInnes, A.G., Walter, J.A., and Wright, J.L.C. (1977). Use of  $^{13}\text{C}$  in biosynthetic studies. Incorporation of  $^{13}\text{C}$ -labeled acetate into chartreusin by *Streptomyces chartreusis*. *Can. J. Chem.* **55**, 2450–2457.
- Chen, Y.H., Wang, C.C., Greenwell, L., Rix, U., Hoffmeister, D., Vining, L.C., Rohr, J., and Yang, K.Q. (2005). Functional analyses of oxygenases in jadomycin biosynthesis and identification of JadH as a bifunctional oxygenase/dehydrase. *J. Biol. Chem.* **280**, 22508–22514.
- Chen, Y., Fan, K., He, Y., Xu, X., Peng, Y., Yu, T., Jia, C., and Yang, K. (2010). Characterization of JadH as an FAD- and NAD(P)H- dependent bifunctional hydroxylase/dehydrase in jadomycin biosynthesis. *ChemBioChem* **11**, 1055–1060.
- Chu, M., Mierzwa, R., Truemees, I., King, A., Patel, M., Berrie, R., Hart, A., Butkiewicz, N., DasMahapatra, B., and Chan, T.-M. (1996). Structure of Sch 68631: a new hepatitis C virus proteinase inhibitor from *Streptomyces* sp. *Tetrahedron Lett.* **37**, 7229–7232.
- Datsenko, K.A., and Wanner, B.L. (2000). One-step inactivation of chromosomal genes in *Escherichia coli* K-12 using PCR products. *Proc. Natl. Acad. Sci. USA* **97**, 6640–6645.
- Ewersmeyer-Wenk, B., Zahner, H., Krone, B., and Zeeck, A. (1981). Metabolic products of microorganisms. 207. Haloquinone, a new antibiotic active against halobacteria. I. Isolation, characterization and biological properties. *J. Antibiot. (Tokyo)* **34**, 1531–1537.
- Farnet, C.M., McAlpine, J.B., Bachmann, B.O., Staffa, A. and Zazopoulos, E. (2008). System, knowledge repository and computer-readable medium for identifying a secondary metabolite from a microorganism. US patent US20080010025 A1, filed October 19, 2006, and published January 10, 2008.
- Flett, F., Mersinias, V., and Smith, C.P. (1997). High efficiency intergeneric conjugal transfer of plasmid DNA from *Escherichia coli* to methyl DNA-restricting streptomycetes. *FEMS Microbiol. Lett.* **155**, 223–229.
- Fritzsche, K., Ishida, K., and Hertweck, C. (2008). Orchestration of discoid polyketide cyclization in the resistomycin pathway. *J. Am. Chem. Soc.* **130**, 8307–8316.
- Fu, H., Ebertkhosla, S., Hopwood, D.A., and Khosla, C. (1994). Engineered biosynthesis of novel polyketides: dissection of the catalytic specificity of the act ketoreductase. *J. Am. Chem. Soc.* **116**, 4166–4170.
- Garrido, L.M., Lombó, F., Baig, I., Nur-e-Alam, M., Furlan, R.L., Borda, C.C., Braña, A., Méndez, C., Salas, J.A., and Rohr, J. (2006). Insights in the glycosylation steps during biosynthesis of the antitumor anthracycline cosmomycin: characterization of two glycosyltransferase genes. *Appl. Microbiol. Biotechnol.* **73**, 122–131.
- Gould, S.J., Melville, C.R., and Chen, J. (1997). The biosynthesis of murayaquinone, a rearranged polyketide. *Tetrahedron* **53**, 4561–4568.
- Gulick, A.M. (2009). Conformational dynamics in the Acyl-CoA synthetases, adenylation domains of non-ribosomal peptide synthetases, and firefly luciferase. *ACS Chem. Biol.* **4**, 811–827.
- Gust, B., Challis, G.L., Fowler, K., Kieser, T., and Chater, K.F. (2003). PCR-targeted *Streptomyces* gene replacement identifies a protein domain needed for biosynthesis of the sesquiterpene soil odor geosmin. *Proc. Natl. Acad. Sci. USA* **100**, 1541–1546.
- Hautala, A., Torkkell, S., Raty, K., Kunnari, T., Kantola, J., Mantsala, P., Hakala, J., and Ylihanko, K. (2003). Studies on a second and third ring cyclization in anthracycline biosynthesis. *J. Antibiot. (Tokyo)* **56**, 143–153.
- Hertweck, C., Luzhetskyy, A., Rebets, Y., and Bechthold, A. (2007). Type II polyketide synthases: gaining a deeper insight into enzymatic teamwork. *Nat. Prod. Rep.* **24**, 162–190.
- Ishida, K., Maksimenka, K., Fritzsche, K., Scherlach, K., Bringmann, G., and Hertweck, C. (2006). The boat-shaped polyketide resistoflavin results from re-facial central hydroxylation of the discoid metabolite resistomycin. *J. Am. Chem. Soc.* **128**, 14619–14624.
- Jackson, D.R., Yu, X., Wang, G., Patel, A.B., Calveras, J., Barajas, J.F., Sasaki, E., Metsä-Ketelä, M., Liu, H.W., Rohr, J., and Tsai, S.C. (2016). Insights into complex oxidation during BE-7585A biosynthesis: structural determination and analysis of the polyketide monooxygenase BexE. *ACS Chem. Biol.* **11**, 1137–1147.
- Kantola, J., Kunnari, T., Hautala, A., Hakala, J., Ylihanko, K., and Mantsala, P. (2000). Elucidation of anthracycline biosynthesis by stepwise cloning of genes for anthracyclines from three different *Streptomyces* spp. *Microbiology* **146**, 155–163.
- Kieser, T., Bibb, M.J., Buttner, M.J., Chater, K.F., and Hopwood, D.A. (2000). *Practical Streptomyces Genetics* (The John Innes Foundation).
- Koskiniemi, H., Metsä-Ketelä, M., Dobritzsch, D., Kallio, P., Korhonen, H., Mäntsälä, P., Schneider, G., and Niemi, J. (2007). Crystal structures of two aromatic hydroxylases involved in the early tailoring steps of angucycline biosynthesis. *J. Mol. Biol.* **372**, 633–648.
- Lario, P.I., Sampson, N., and Vrielink, A. (2003). Sub-atomic resolution crystal structure of cholesterol oxidase: what atomic resolution crystallography reveals about enzyme mechanism and the role of the FAD cofactor in redox activity. *J. Mol. Biol.* **326**, 1635–1650.
- Luo, M., and Wing, R.A. (2003). An improved method for plant BAC library construction. *Methods Mol. Biol.* **236**, 3–20.
- Maier, S., Pfluger, T., Loesgen, S., Asmus, K., Brotz, E., Paululat, T., Zeeck, A., Andrade, S., and Bechthold, A. (2014). Insights into the bioactivity of mensacarcin and epoxide formation by MsnO8. *ChemBioChem* **15**, 749–756.
- Maier, S., Heitzler, T., Asmus, K., Brotz, E., Hardter, U., Hesselbach, K., Paululat, T., and Bechthold, A. (2015). Functional characterization of different ORFs including luciferase-like monooxygenase genes from the mensacarcin gene cluster. *ChemBioChem* **16**, 1175–1182.
- Marchler-Bauer, A., Bo, Y., Han, L., He, J., Lanczycki, C.J., Lu, S., Chitsaz, F., Derbyshire, M.K., Geer, R.C., Gonzales, N.R., et al. (2016). CDD/SPARCLE: functional classification of proteins via subfamily domain architectures. *Nucleic Acids Res.* **45**, D200–D203.
- McDaniel, R., Ebert-Khosla, S., Fu, H., Hopwood, D.A., and Khosla, C. (1994). Engineered biosynthesis of novel polyketides: influence of a downstream enzyme on the catalytic specificity of a minimal aromatic polyketide synthase. *Proc. Natl. Acad. Sci. USA* **91**, 11542–11546.
- Melville, C.R., and Gould, S.J. (1994). Murayalactone, a dibenzo- $\alpha$ -pyrone from *Streptomyces murayamaensis*. *J. Nat. Prod.* **57**, 597–601.
- Murooka, Y., and Yamashita, M. (2001). Genetic and protein engineering of diagnostic enzymes, cholesterol oxidase and xylitol oxidase. *J. Biosci. Bioeng.* **91**, 433–441.
- Pickens, L.B., Kim, W., Wang, P., Zhou, H., Watanabe, K., Gomi, S., and Tang, Y. (2009). Biochemical analysis of the biosynthetic pathway of an anticancer tetracycline SF2575. *J. Am. Chem. Soc.* **131**, 17677–17689.
- Polonsky, J., and Lederer, E. (1963). Piloquinone: a new phenanthrene- $o$ -quinone isolated from the mycelium of *Streptomyces pilosus*. *Nature* **199**, 285–286.
- Rix, U., Wang, C., Chen, Y., Lipata, F.M., Rensing Rix, L.L., Greenwell, L.M., Vining, L.C., Yang, K., and Rohr, J. (2005). The oxidative ring cleavage in jadomycin biosynthesis: a multistep oxygenation cascade in a biosynthetic black box. *ChemBioChem* **6**, 838–845.
- Robbins, T., Liu, Y.C., Cane, D.E., and Khosla, C. (2016). Structure and mechanism of assembly line polyketide synthases. *Curr. Opin. Struct. Biol.* **41**, 10–18.
- Sasaki, E., Ogasawara, Y., and Liu, H.-W. (2010). A biosynthetic pathway for BE-7585A, a 2-thiosugar-containing angucycline-type natural product. *J. Am. Chem. Soc.* **132**, 7405–7417.
- Sato, Y., Kohnert, R., and Gould, S.J. (1986). Application of long range  $^1\text{H}/^{13}\text{C}$  heteronuclear correlation spectroscopy (LR HETCOSY) to structure elucidation: the structure of murayaquinone. *Tetrahedron Lett.* **27**, 143–146.

- Shen, B., and Hutchinson, C.R. (1994). Triple hydroxylation of tetracenomyacin A2 to tetracenomyacin C in *Streptomyces glaucescens*. Overexpression of the tcmG gene in *Streptomyces lividans* and characterization of the tetracenomyacin A2 oxygenase. *J. Biol. Chem.* *269*, 30726–30733.
- Snapper, S.B., Melton, R.E., Mustafa, S., Kieser, T., and Jacobs, W.R., Jr. (1990). Isolation and characterization of efficient plasmid transformation mutants of *Mycobacterium smegmatis*. *Mol. Microbiol.* *4*, 1911–1919.
- Tibrewal, N., Pahari, P., Wang, G., Kharel, M.K., Morris, C., Downey, T., Hou, Y., Bugni, T.S., and Rohr, J. (2012). Baeyer-Villiger C-C bond cleavage reaction in gilvocarcin and jadomycin biosynthesis. *J. Am. Chem. Soc.* *134*, 18181–18184.
- Trefzer, A., Hoffmeister, D., Kunzel, E., Stockert, S., Weitnauer, G., Westrich, L., Rix, U., Fuchser, J., Bindseil, K.U., Rohr, J., and Bechthold, A. (2000). Function of glycosyltransferase genes involved in urdamycin A biosynthesis. *Chem. Biol.* *7*, 133–142.
- Walsh, C.T. (2016). Insights into the chemical logic and enzymatic machinery of NRPS assembly lines. *Nat. Prod. Rep.* *33*, 127–135.
- Xu, Z., Jakobi, K., Welzel, K., and Hertweck, C. (2005). Biosynthesis of the anti-tumor agent chartreusin involves the oxidative rearrangement of an anthracyclic polyketide. *Chem. Biol.* *12*, 579–588.
- Xu, M., Wang, Y., Zhao, Z., Gao, G., Huang, S.X., Kang, Q., He, X., Lin, S., Pang, X., Deng, Z., and Tao, M. (2016). Functional genome mining for metabolites encoded by large gene clusters through heterologous expression of a whole-genome bacterial artificial chromosome library in *Streptomyces* spp. *Appl. Environ. Microbiol.* *82*, 5795–5805.
- Yue, Q.K., Kass, I.J., Sampson, N.S., and Vrielink, A. (1999). Crystal structure determination of cholesterol oxidase from *Streptomyces* and structural characterization of key active site mutants. *Biochemistry* *38*, 4277–4286.
- Zhan, J. (2009). Biosynthesis of bacterial aromatic polyketides. *Curr. Top. Med. Chem.* *9*, 1958–610.
- Zhang, W., Watanabe, K., Wang, C.C., and Tang, Y. (2007). Investigation of early tailoring reactions in the oxytetracycline biosynthetic pathway. *J. Biol. Chem.* *282*, 25717–25725.
- Zhu, T., Cheng, X., Liu, Y., Deng, Z., and You, D. (2013). Deciphering and engineering of the final step halogenase for improved chlortetracycline biosynthesis in industrial *Streptomyces aureofaciens*. *Metab. Eng.* *19*, 69–78.

## STAR★METHODS

### KEY RESOURCES TABLE

REAGENT or RESOURCE	SOURCE	IDENTIFIER
<b>Bacterial and Virus Strains</b>		
<i>E. coli</i> : DH10B	Gibco BRL	Cat#19625011
<i>E. coli</i> : ET12567/pUB307	Flett et al., 1997	N/A
<i>E. coli</i> : BW25113/pIJ790	Datsenko and Wanner, 2000; Gust et al., 2003	N/A
<i>E. coli</i> : BT340	Gust et al., 2003	N/A
<i>E. coli</i> : BL21(DE3)	Agilent Technologies	Cat#200131
<i>E. coli</i> : BL21(DE3)/pGro7	TAKARA	Cat#9122
<i>S. griseoruber</i> Sgr29	CCTCC	AA94052
<i>S. lividans</i> : SBT5	Bai et al., 2014	N/A
<i>S. lividans</i> : SBT5::3B4	This paper	N/A
<i>S. lividans</i> : SBT5::2E12	This paper	N/A
<i>S. lividans</i> : SBT5::6F3	This paper	N/A
<i>S. lividans</i> : SBT5::3B4Δpks	This paper	N/A
<i>S. lividans</i> : SBT5::3B4Δright	This paper	N/A
<i>S. lividans</i> : SBT5::3B4Δleft	This paper	N/A
<i>S. lividans</i> : SBT5::3B4Δorf-2	This paper	N/A
<i>S. lividans</i> : SBT5::3B4Δorf-1	This paper	N/A
<i>S. lividans</i> : SBT5::3B4ΔRT	This paper	N/A
<i>S. lividans</i> : SBT5::3B4Δorf(1-22)	This paper	N/A
<i>S. lividans</i> : SBT5::3B4Δorf23	This paper	N/A
<i>S. lividans</i> : SBT5::3B4Δorf24	This paper	N/A
<i>S. lividans</i> : SBT5::3B4ΔmrqO8	This paper	N/A
<i>S. lividans</i> : SBT5::3B4ΔmrqM	This paper	N/A
<i>S. lividans</i> : SBT5::3B4ΔmrqO1	This paper	N/A
<i>S. lividans</i> : SBT5::3B4ΔmrqD	This paper	N/A
<i>S. lividans</i> : SBT5::3B4ΔmrqE	This paper	N/A
<i>S. lividans</i> : SBT5::3B4ΔmrqF	This paper	N/A
<i>S. lividans</i> : SBT5::3B4ΔmrqO2	This paper	N/A
<i>S. lividans</i> : SBT5::3B4ΔmrqG	This paper	N/A
<i>S. lividans</i> : SBT5::3B4ΔmrqO3	This paper	N/A
<i>S. lividans</i> : SBT5::3B4ΔmrqO4	This paper	N/A
<i>S. lividans</i> : SBT5::3B4ΔmrqH	This paper	N/A
<i>S. lividans</i> : SBT5::3B4ΔmrqI	This paper	N/A
<i>S. lividans</i> : SBT5::3B4ΔmrqJ	This paper	N/A
<i>S. lividans</i> : SBT5::3B4ΔmrqK	This paper	N/A
<i>S. lividans</i> : SBT5::3B4ΔmrqO5	This paper	N/A
<i>S. lividans</i> : SBT5::3B4ΔmrqO6	This paper	N/A
<i>S. lividans</i> : SBT5::3B4ΔmrqO7	This paper	N/A
<i>S. lividans</i> : SBT5::3B4ΔmrqL	This paper	N/A
<i>Staphylococcus aureus</i>	ATCC	ATCC25923
<i>Mycobacterium smegmatis</i> mc <sup>2</sup> 155	Snapper et al., 1990	N/A
<b>Biological Samples</b>		
Plasmid: pHL921	Xu et al., 2016	N/A
Plasmid: pET-28a	Novagen	Cat#69864-3
Plasmid: pJTU6722	This paper	N/A

(Continued on next page)

### Continued

REAGENT or RESOURCE	SOURCE	IDENTIFIER
BAC clone: 2E12	This paper	N/A
BAC clone: 3B4	This paper	N/A
BAC clone: 6F3	This paper	N/A
Critical Commercial Assays		
Bradford Protein Assay Kit	TIANGEN BIOTECH (BEIJING) CO.,LTD	Cat#PA102
Fluorimetric Hydrogen Peroxide Assay Kit	Sigma Aldrich	Cat#MAK 166
Deposited Data		
<i>mrq</i> gene cluster	This paper	GenBank: KX817190
Oligonucleotides		
proO3-F: GGAATTCATATGATGAAACCCATCAG CAC	This paper	N/A
proO3-R: GTATACCGCTCGAGTCAGCGGCCG CGACCGA	This paper	N/A
proO6-F: GAATTCATATGTCCGAGGCGACCGTGC CCGT	This paper	N/A
proO6-R: ATACCGCTCGAGTCAGCCCGCGGGCG GTCCAGGA	This paper	N/A
proO7-F: GGAATTCATATGACGATCGTGGTGACC GGGGCC	This paper	N/A
proO7-R: CCCAAGCTTCAGGCGAAGTGCGGGCG TGGGC	This paper	N/A

## CONTACT FOR REAGENT AND RESOURCE SHARING

Further information and requests for resources and reagents should be directed to and will be fulfilled by the Lead Contact, Meifeng Tao ([tao\\_meifeng@sjtu.edu.cn](mailto:tao_meifeng@sjtu.edu.cn)).

## EXPERIMENTAL MODEL AND SUBJECT DETAILS

### Bacterial Strains

*E. coli* DH10B was used as a host for general cloning and construction of the genomic BAC library. *E. coli* BW25113/pIJ790 (Datsenko and Wanner, 2000; Gust et al., 2003) was used for  $\lambda$ -red mediated recombination to construct deletion mutants. *E. coli* BT340 (i.e. DH5 $\alpha$ /pCP20) was used for construction of in-frame deletion employing FLP-mediated site-specific recombination (Gust et al., 2003). *E. coli* ET12567/pUB307 was used as a helper strain for *E. coli*-*Streptomyces* inter-genus conjugation (Flett et al., 1997). *S. griseoruber* Sgr29 was obtained from China Center for Type Culture Collection (CCTCC). *S. lividans* SBT5 (Bai et al., 2014) was used as a host for heterologous expression of the whole BAC library and BAC clones carrying the wild type *mrq* gene cluster and its deleted variants. *Staphylococcus aureus* and *Mycobacterium smegmatis* mc<sup>2</sup>155 (Snapper et al., 1990) were used as indicators for bioassay.

### Plasmids

pHL921 carrying an origin of transfer (*oriT*), an integrase gene (*int*), and a site of integration (*attP<sup>φC31</sup>*) was used as a BAC vector. pHL921-derived plasmids (BAC clones) can be mobilized into *Streptomyces* and integrate in the chromosomal attachment site (*attB<sup>φC31</sup>*) (Xu et al., 2016). pJTU6722 carrying an FRT-*eryB*-FRT cassette, i.e. erythromycin-resistance gene *ermB* flanked by a FLP recombination target site (FRT) at either sides, was used for gene inactivation by  $\lambda$ -red-mediated recombination. pET-28a (Novagen) was used for protein expression.

### Culture Conditions

Lysogeny broth (LB) medium was used for *E. coli* growth. MS medium (Kieser et al., 2000) was used for *Streptomyces* growth, sporulation, and conjugation. No18 agar medium (glycerol 2%, cane molasses 1%, casamino acids 0.5%, peptone 0.1%, CaCO<sub>3</sub> 0.4%, agar 2%, pH 7.0) (Farnet et al., 2008) was used for fermentation. *Streptomyces* and *E. coli* BT340 were grown at 30°C.

## METHODS DETAILS

### Construction and Screen of the Genomic BAC Library of *S. griseoruber* Sgr29

Large fragment genomic DNA was extracted from *S. griseoruber* Sgr29 and used to construct a genomic BAC library according to a previous protocol (Luo and Wing, 2003) in *E. coli* DH10B, yielding a library with 912 clones and an average insertion of ca. 100 kb. The library was stored in 96-well plates.

BAC clones carrying the *mrq* gene cluster were identified using the LEXAS technology (Xu et al., 2016). Briefly, the whole library was grown in LB broth (100  $\mu$ L/well) for 6–8 h at 37°C in 96-well plates to OD<sub>600</sub> about 0.6. The conjugation helper strain *E. coli* ET12567/pUB307 was grown in LB with kanamycin at final concentration of 50  $\mu$ g/mL for 6 h at 37°C to OD<sub>600</sub> 0.6, harvested, washed, and resuspended in 1/10 volume of LB. ET12567/pUB307 was then added to each well (10  $\mu$ L/well) of the 96-well plates and mixed. The conjugation recipient *S. lividans* SBT5 spores were flooded onto MS agar at ca. 10<sup>8</sup> colony-forming units/9-cm Petri dish. Then the DH10B/BACs-ET12567/pUB307 mixtures in 96-well plates were transferred to the spores-coated Petri dishes by stamping with a 48-pin inoculator. The inoculated Petri dishes were incubated at 30°C for 12–16 h and flooded with 1 mL antibiotic solution of apramycin (to select for exconjugants) and trimethoprim (to select against *E. coli* cells). After incubation at 30°C for 7 d, the apramycin-resistant *S. lividans* SBT5 exconjugants were transferred to fresh MS plates containing apramycin and trimethoprim, incubated at 30°C for 7 d, the exconjugants were finally transferred to No18 agar plates for micro-fermentation. After 7 days of fermentation at 30°C, each plates of fermented exconjugants was flooded with LB (supplemented with 0.5% agar) containing indicators (*Staphylococcus aureus* or *Mycobacterium smegmatis* mc<sup>2</sup>155) and incubated at 37°C for 12–20 h. Inhibitory zones could be observed.

### Construction of Large Deletion Mutants and Single Gene Deletion Mutants

Gene deletion mutants were constructed on the BAC clone 3B4 by  $\lambda$ -red mediated PCR targeting technology (Gust et al., 2003). The amplified products were purified and transformed into *E. coli* BW25113/pLJ790/3B4 competent cells by electroporation to replace a targeted fragment or single gene in 3B4 respectively, yielding replacement constructs. For construction of in-frame deletion, the replacement constructs were introduced to *E. coli* BT340 and cultured at 42°C to remove the FRT-*eryB*-FRT cassette by FLP-mediated excision with an 81 bp scar left. The resulted constructs were confirmed by PCR analyses. The constructs were introduced into *S. lividans* SBT5 individually by tri-parental mating, yielding different deletion mutants.

### Purification of Compounds 1–3 from *S. lividans* SBT5/3B4

*S. lividans* SBT5/3B4 was fermented (on 10 L No18 agar medium) and the culture was extracted with equal volume methanol for three times. The resulting crude extract was concentrated by evaporation, suspended in 5 L water, and adjusted to pH 7.0. The resulting water phase was extracted with ethyl acetate (EtOAc). The organic phase was collected and evaporated. The extract was re-dissolved and subjected to silica gel column chromatography, and eluted with a petroleum ether-EtOAc-CH<sub>3</sub>OH system. Fractions containing **2** were subjected to C18 reverse phase silica gel column chromatography eluted by CH<sub>3</sub>OH-H<sub>2</sub>O system, yielding 14 mg pure **2**. Fractions containing **3** and **1** were subjected to silica gel column chromatography eluted with a CH<sub>2</sub>Cl<sub>2</sub>-CH<sub>3</sub>OH system to separate **3** and **1**. Fractions containing **3** were collected, concentrated, dissolved in CH<sub>3</sub>OH, loaded on Sephadex LH-20 column, and eluted with CH<sub>3</sub>OH. 12 mg pure **3** was obtained. Fractions containing **1** were purified by semipreparative HPLC to yield 8 mg pure **1**.

### Purification of Compounds 4 and 5 from *S. lividans* SBT5/3B4 $\Delta$ *mrqO4*

Fermented culture of *S. lividans* SBT5/3B4 $\Delta$ *mrqO4* (10 L) were extracted with acetone. The resulting crude extract were concentrated by evaporation, suspended in 5 L water, and adjusted to pH 7.0. The water phase was extracted with ethyl acetate, and the resulting organic phase was dried by evaporation. The resultant residue was re-dissolved and subjected to silica gel column chromatography eluted with a petroleum ether-EtOAc-CH<sub>3</sub>OH system. Fractions containing compound **4** were subjected to a silica gel column chromatography eluted by a petroleum ether-CH<sub>2</sub>Cl<sub>2</sub> system, yielding 12 mg compound **4**. Fractions containing compound **5** were subjected to a C18 reverse phase silica gel column chromatography eluted by a CH<sub>3</sub>OH-H<sub>2</sub>O system to give fractions containing compound **5**. After a silica gel column chromatography eluted by a petroleum ether-CH<sub>2</sub>Cl<sub>2</sub> system, 12 mg pure compound **5** was obtained.

### Purification of Compound 6 from *S. lividans* SBT5/3B4 $\Delta$ *mrqO7*

Fermented culture of *S. lividans* SBT5/3B4 $\Delta$ *mrqO7* (5 L) was extracted with acetone and the crude extract was concentrated, suspended in 3 L water, and adjusted to pH 7.0. The water phase was extracted with ethyl acetate, the organic phase was collected, dried by evaporation. The resultant residues were re-dissolved and subjected to silica gel column chromatography eluted with a CH<sub>2</sub>Cl<sub>2</sub>-CH<sub>3</sub>OH elution system. Compound **6** was eluted from the silica gel when the CH<sub>2</sub>Cl<sub>2</sub>:CH<sub>3</sub>OH ratio was of 100:3. Fractions containing compound **6** were combined, dried by evaporation, and further purified by semipreparative chromatography at a flow rate of 2 mL/min on an Agilent ZORBAXSB-C18 column (5  $\mu$ m, 9.4 mm  $\times$  250 mm) eluted by 75% MeOH for 25 min. The eluent should be evaporated as soon as possible since compound **6** was unstable in solution. 12 mg compound **6** was obtained.

### In Vivo Conversion of 6 to 1 by Feeding 6 to Mutants during Fermentation

*S. lividans* strains SBT5/3B4 $\Delta$ *pks*, SBT5/3B4 $\Delta$ *mrqE*, SBT5/3B4 $\Delta$ *mrqF*, SBT5/3B4 $\Delta$ *mrqG*, SBT5/3B4 $\Delta$ *mrqM*, SBT5/3B4 $\Delta$ *mrqO3*, SBT5/3B4 $\Delta$ *mrqO4*, SBT5/3B4 $\Delta$ *mrqO5* and the wild type SBT5/3B4 were fermented on No18 agar medium (in 9-cm Petri dishes)

at 30°C. Each dish was flooded with 30 mg compound **6** dissolved in 1 mL methanol : water (1:1) after 3 days of incubation, and incubated for a further 3 days. The culture in each plate was extracted by ethyl acetate, dried by evaporation, dissolved in 0.5 mL methanol, and 20  $\mu$ L sample was subjected to HPLC detection.

#### Feeding **4** to the $\Delta$ *pks* Mutant during Fermentation

*S. lividans* strains SBT5/3B4 $\Delta$ *pks* and the wild type SBT5/3B4 were fermented in 50 mL No18 liquid medium (in 250 mL flask) at 30°C, 220 rpm. Each flask was added with 10 mg compound **4** dissolved in 1.5 mL methanol:CH<sub>2</sub>Cl<sub>2</sub> (2:1) after 3 days of incubation, and incubated for a further 3 days. The culture in each flask was extracted by ethyl acetate, dried by evaporation, dissolved in 1 mL methanol, and 20  $\mu$ L sample was subjected to HPLC detection.

#### Expression, Purification and Analysis of MrqO3, MrqO6 and MrqO7

*mrqO3*, *mrqO6*, and *mrqO7* were amplified from BAC 3B4 using primer pairs proO3-F/proO3-R, proO6-F/proO6-R, and proO7-F/proO7-R, inserted into pET28a at either NdeI-XhoI or NdeI-HindIII sites, so as to allow the expression of recombinant proteins with an N-terminal His(6) tag. MrqO6 and MrqO7 were produced in *E. coli* BL21(DE3) while MrqO3 was produced in *E. coli* strain BL21(DE3)/pGro7. The three proteins were expressed and purified in a similar manner. *E. coli* cultures (200 mL, in LB with kanamycin 50  $\mu$ g/mL) were grown at 37°C to OD<sub>600</sub> ~0.6, induced by addition of 0.4 mM IPTG and followed by overnight growth (~18 h) at 16°C. Following incubation, cultures were harvested and the cell pellets were resuspended in 30 mL 50 mM Tris-HCl buffer (50 mM Tris, 150 mM NaCl, pH 7.5, glycerol 10%). Cells were lysed by repeated sonication, the lysate was centrifuged at 12,000 rpm for 25 min, and the resulting supernatant was added to a gravity-flow column containing 1 mL Ni<sup>2+</sup> metal-chelate affinity resin (Bio-Rad). For the purification of MrqO3, the resin was washed with 10 mL 50 mM Tris-HCl supplemented with 30 mM imidazole to remove unspecifically bound protein. For MrqO6, the resin was washed with 10 mL 50 mM Tris-HCl supplemented with 40 mM imidazole. For MrqO7, the resin was washed with 10 mL 50 mM Tris-HCl supplemented with 50 mM imidazole. Then 5 mL 50 mM Tris-HCl supplemented with 500 mM imidazole were applied to the column to elute His-tagged proteins. PD-10 desalting columns were used to remove imidazole in the protein eluents. The desalted eluents were applied to Amicon Ultra-15 millipores (10 kDa, Merck) to concentrate the proteins. The concentrations of the proteins were determined by microplate reader using the Protein Bradford Assay Kit (Tiangen Biotech Company). The purified proteins were used for the in vitro enzyme activity assays.

#### Determination of the Catalytic Order of MrqO6 and MrqO7

Three sequential-reactions were conducted to determine the catalytic order of MrqO6 and MrqO7. These reactions were set up to 250  $\mu$ L with 246  $\mu$ M compound **6** and 1 mM NADPH and run in a two-step manner with the first step incubated for 45 min at 30°C, the protein removed by Amicon Ultra-15 millipore (10 kD, Merck), and followed by the second step incubated for 1 h at 30°C. In sequential-reaction I, MrqO7 (2  $\mu$ M) was added for the first step reaction, and MrqO6 and MrqO3 (2  $\mu$ M each) were added for the second step reaction. In sequential-reaction II, MrqO6 (2  $\mu$ M) was added for the first step reaction, and MrqO7 and MrqO3 (2  $\mu$ M each) were added for the second step reaction. In sequential-reaction III, no enzyme was added for the first step, and three enzymes MrqO7, MrqO6 and MrqO3 (2  $\mu$ M each) were added for the second step reaction. After incubation, each reaction mixture was extracted with CH<sub>2</sub>Cl<sub>2</sub>, the organic phase was collected, air dried, dissolved with 20  $\mu$ L MeOH, and detected by HPLC at 280 nm.

#### Detection of H<sub>2</sub>O<sub>2</sub> in the In Vitro Conversion of **6** to **1** Catalyzed by MrqO7, MrqO6 and MrqO3

H<sub>2</sub>O<sub>2</sub> was detected using the Fluorimetric Hydrogen Peroxide Assay Kit (Catalog Number MAK166, Sigma) according to the product instruction. A liner standard curve was generated in the range of 0-10  $\mu$ M H<sub>2</sub>O<sub>2</sub> and R<sup>2</sup> of the standard curve is 0.99776. The in vitro enzymatic assays were performed with 2  $\mu$ M each enzyme, 1 mM NADPH, and 360  $\mu$ M **6**. The assay mixtures were incubated at 30°C for 20 min, then three samples of 10  $\mu$ L, 20  $\mu$ L and 30  $\mu$ L were taken for the detection of H<sub>2</sub>O<sub>2</sub>. Meanwhile, the assay mixtures were extracted by CH<sub>2</sub>Cl<sub>2</sub>. The resultant organic phases were dried and resolved in 20  $\mu$ L methanol for HPLC analysis, confirming the conversion of **6** to **1** in the in vitro assays.

#### QUANTIFICATION AND STATISTICAL ANALYSIS

See individual sections above and legends of pictures for details on the statistics used for analysis.

#### DATA AND SOFTWARE AVAILABILITY

##### Data Resources

The *mrq* gene cluster reported in this paper has been deposited in the NCBI under the accession number GenBank: KX817190.